

## Case Report

# Identification of novel compound heterozygosity variants in *GPD1* causing infantile transient hypertriglyceridemia

Yi Long, Xianhua Zhang, Ping Gong, Bing Zhang, Xian Hu, Lina Yang

Children's Medical Center, Hunan Provincial People's Hospital/The First Affiliated Hospital of Hunan Normal University, Changsha, Hunan, P. R. China

Received February 26, 2018; Accepted June 28, 2018; Epub December 15, 2018; Published December 30, 2018

**Abstract:** Background: Transient infantile hypertriglyceridemia (HTGT1) is a rare autosomal recessive disorder caused by dysfunction of glycerol-3-phosphate dehydrogenase 1 (GPD1) and is characterized by early-onset transient hypertriglyceridemia. Methods: Liver biopsy was performed with IHC, histopathology was done with special staining for Masson trichrome test, and electron microscopy was performed. Whole exome sequencing (WES) of the proband led to prioritized candidate genes based on clinical, pedigree, and mutation characteristics, and mutations were validated by Sanger sequencing. Results: The proband had hepatosplenomegaly, and liver biopsy pathology confirmed non-alcoholic steatohepatitis. The whole exome sequencing for the proband identified a compound heterozygote in *GPD1* gene, containing c.806G>A (p.R269Q) and c.220-2A>G of NM\_0052763. Further analysis showed the two mutations were inherited from his father and mother, respectively. Conclusions: In conclusion, our study found the etiology for a patient with HTGT1 by using whole exome sequencing. These data demonstrate the potential of WES for diagnosis of monogenic disease.

**Keywords:** Transient infantile hypertriglyceridemia, *GPD1* gene, compound heterozygote, whole exome sequencing

### Introduction

Transient infantile hypertriglyceridemia (HTGT1) is a rare autosomal recessive disorder and is characterized by early-onset transient hypertriglyceridemia. The disease is caused by dysfunction of glycerol-3-phosphate dehydrogenase 1 (GPD1). To date, 5 mutations in *GPD1* gene, such as p.C214R, p.R229Q, p.R229P, p.R269Q and c.361-1G>C, have been found to be associated with HTGT1 and 15 patients have been reported. Interestingly, the 15 patients have had various phenotypes, suggesting HTGT1 is a heterogeneous disorder. The common complications of HTGT1 comprise hepatomegaly and hepatic steatosis. In a Caucasian female infant with HTGT1, failure to thrive, vomiting, and an enlarged abdomen were also observed [1]. Another previous study reported 3 patients with different common complications. One patient had recurrent episodes of fasting hypoglycemia, the second showed intrahepatic cholestasis associated with kidney involve-

ment, and the third presented with persistent hypertriglyceridemia at 30 years of age [2].

GPD1 catalyzes the reversible redox reaction of dihydroxyacetone phosphate (DHAP) and reduced nicotinic adenine dinucleotide (NADH) to glycerol-3-phosphate (G3P) and NAD<sup>+</sup>. G3P is important for synthesis of triglycerides. In addition, together with a mitochondrial isoform, GPD2, GPD1 plays an important role in the transport of reducing equivalents from the cytosol to the mitochondria [3]. Brown et al. (2002) stated that mice lacking cytosolic GPD are phenotypically normal, although they have metabolic abnormalities in certain tissues. They found that mice lacking both cytosolic and mitochondrial GPD (GPD2) were active and nursed well for several days, but they failed to grow and usually died within the first week [4]. These mice shared some features of both glycerol kinase deficiency and hereditary fructose intolerance, suggesting the phenotype resulted from the combined effects of the loss of glu-

## GPD1 causing transient hypertriglyceridemia

coneogenic substrate, the osmotic effects of glycerol, and the metabolic effects of accumulated phosphorylated metabolites [4].

To date, HTGT1 has been found in many populations, such as the Israeli-Arab, Caucasian, and Italian populations. Here, we identified a proband via WES in a Chinese patient who suffered from HTGT1. Our report expands the molecular spectrum of mutations underlying HTGT1 and their associated clinical phenotypes.

### Materials and methods

#### *Patient*

The patient, a 5-month-old boy, was admitted to our department due to obvious abdominal distension revealed by the parents 5 days before hospitalization. He was the first and only child of a non-consanguineous Chinese couple, born at full-term gestation following an uncomplicated pregnancy, with a birth weight of 3.6 kg and length of 50 cm. Jaundice was noted 3 days after birth and was cured after treated for two and a half months. A history of hepatitis, tuberculosis, malaria, trauma, surgery, and blood transfusion were all denied. His psychological condition was normal ever since the onset, and no vomiting, cough, or fever was noted. No significant body weight change was found. The present study was approved by the Ethics Committee of Hunan Provincial People's Hospital, and informed consent was obtained from the parents of the patient.

#### *Liver biopsy, immunohistochemistry (IHC), and electron microscopy*

After antisepsis and anesthesia, liver biopsy was performed under the guidance of Doppler ultrasound with the puncture point on costal margin. The tissue was then applied for pathological examination. Briefly, the specimen was fixed with 4% paraformaldehyde, embedded in paraffin, and sliced continuously into about 4  $\mu$ m sections. Immunohistochemical staining was then performed with EnVision two-step method. As for transmission electron microscope, a 1 mm diameter liver biopsy was cut with a sharp knife, fixed and cleaned with pre-cooled with 2.5% glutaraldehyde, fixed and cleaned with 1% OsO<sub>4</sub>, washed, dehydrated with gradient alcohol-acetone, infiltrated with resin, embedded, ultra-thin section, uranium and lead double staining, and observed with

JEM-1400 PLUS transmission electron microscope.

#### *Whole exome sequencing*

WES was undertaken using Illumina HiSeq2500 (Illumina, Santiago, USA). Briefly, 2 ml peripheral blood was collected from the family trio. Genomic DNA was extracted from leukocytes, followed by library construction and sequencing. The sequencing reads were aligned to the human reference genome (hg19) using BWA after the raw data were processed. MuTect (single-nucleotide variants, SNVs), genome analysis toolkit (GATK) [5], and Annovar [6] were allied for variant calling. Filtration was undertaken by 1000 genomes project database, dbSNP, ESP, and Exac database with a 0.5% frequency cut-off. Non-synonymous, loss-of-function, indel, duplication, and splice site variants were performed for candidate variants identification. Proven [7], MutationAssessor [8], and PolyPhen-2 [9] were enrolled for biological function prediction.

#### *Sanger sequencing*

Sanger sequencing was applied for the family members using genomic DNA extracted from peripheral blood. The sequences containing the variants in *GPD1* gene were amplified. The primers were designed with PerlPrimer software (<http://perlprimer.sourceforge.net/>). The primers used were as following: GPD1-1-F: 5'-TCCAAGTTCAGTCCTTCTAGATTC-3', reverse, GPD1-1-R: 5'-AACAAACTGCCATTCAGTGACCA-3'; GPD1-2-F: 5'-GATCAACTAGAGAGAAGAGTGGT-3', reverse, GPD1-2-R: 5'-TCTGGACTCTGTCTGAAATGTAAG-3', with the products of 628 bp and 947 bp in length. Amplification was performed with annealing temperature of 60°C. The PCR products were sequenced with ABI 3730XL (Thermo Fisher Scientific Inc, Waltham, USA) and analyzed by DNASTAR 5.0 software (DNASTAR, Inc, Madison, USA).

#### *Gene expression profile analysis in human and phenotype-gene analysis*

The online service GeneFriends database (<http://www.genefriends.org/>) was used for finding co-expressed genes with *GPD1* [10]. The genes with the value of Pearson Correlation higher than 0.75 were considered to be co-expressed. Protein-protein interactions (PPI) were analyzed in string-db (<https://string-db>).

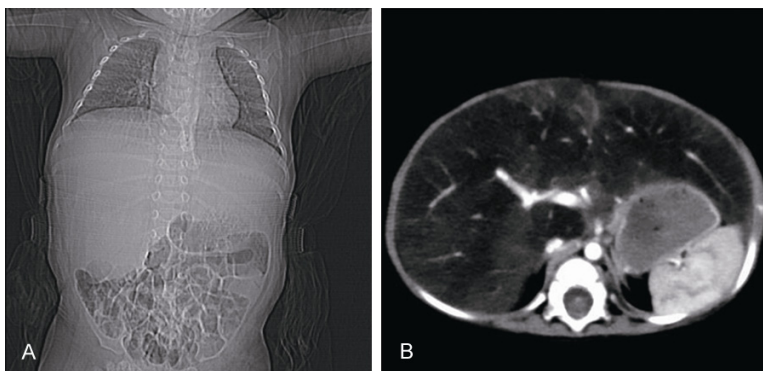


**Figure 1.** The results of doppler color ultrasonography. A. Enlarged parenchyma and diffuse parenchymal lesions were found in liver. B. Bright spots were found in both kidney.

org/) [11] and their enrichment were analyzed with GeneTrail2 (<https://genetrail2.bioinf.uni-sb.de/>) [12].

## Results

### Laboratory examinations

In order to make conclusive diagnosis, laboratory examination was performed. Blood routine: WBC  $16.08 \times 10^9/L$ , N 18.0%, L 73.2%, E 1.4%, RBC  $4.77 \times 10^{12}/L$ , HGB 124 g/l, and Plt  $244 \times 10^9/L$ . Blood gas analysis results were as follows: pH 7.41,  $pCO_2$  18,  $pO_2$  100.3,  $HCO_3$  11.4, BE -10.3, and  $SO_2$  97.9%. Blood lipids and liver function detective results were: TCHOL 2.56 mmol/L, TG 4.41 mmol/L, HDL 0.7 mmol/L, LDL 1.27 mmol/L, APOA 1.19 mmol/L, APOB 0.90 mmol/L, ALT 69.3 U/L, AST 102.5 U/L, and GGT 159.8 U/L. Tests including coagulation function, stool routine, blood sugar, blood ammonia, copper blue protein, blood and urine CMV-DNA and CMV-pp65, HBV, HEV, blood culture, and bone marrow cytology were all negative. Metabolic screening of blood and urine excluded the existence of genetic disorders in typical amino acids, organic acids, and fatty acids metabolism. Collectively, the decrease of TCHOL and HDL and the increase of TG, ALT, AST and GGT, were consistent with the biochemical performance of nonalcoholic fatty liver disease (NAFLD) patients [13].

### Nonalcoholic steatohepatitis revealed by liver biopsy

To further identify the abdominal diseases, doppler color ultrasonography was undertaken.

The result demonstrated enlarged liver parenchyma and diffuse liver parenchymal lesions and hyperechogenic kidneys were also found (**Figure 1**).

In order to illustrate the damage of the liver, biopsy was performed with IHC, histopathology special stain masson trichrome test, and electron microscopy. Some of the confluence areas were slightly enlarged, with a small amount of lymphocytic infiltration and mild hyperplasia of fibrous tissue (**Figure 2A** and **2B**).

Diffuse hepatic steatosis was noted, with the steatosis in excess of 90% and partial focal necrosis. No Mallory corpuscles or interface inflammation was found (**Figure 2C**). There was no obvious dilatation in interlobular vein and hepatic sinusoid. No obvious edema and inflammatory cell infiltration in the central venous membrane were identified (**Figure 2**). Together, the results argued for nonalcoholic steatohepatitis in the liver.

### Detection of pathogenic variants

In order to identify potential molecular pathogeny, WES was performed. The percentage of coverage and average depth of the proband for WES were 99.5% and 94.2X. More than 95% of the sequencing reads were aligned to the human reference genome (hg19), with more than 86.00% of target regions having at least a 10-fold coverage. As a result, 20,171 SNVs and InDels were identified. After filtering with coding sequence, rare mutations with allele frequency  $<0.001$  based on Exome Aggregation Consortium (ExAC), 1000 Genomes and the NHLBI Exome Sequencing Project (ESP) were identified. Then “pathogenic” mutations, according to the ACMG guideline, were retained [14]. Finally, the proband was found to be a compound heterozygote in the GPD1 gene, containing c.806G>A (p.R269Q) and c.220-2A>G of NM\_0052763. A previous study found that the c.220-2A>G variant generates an aberrant splicing, results in a truncated exon 3, so, the first 69 bases in exon 3 are lost (c.220\_288del), and finally leads to the deletion of 23 amino acids from the GPD1 protein

## GPD1 causing transient hypertriglyceridemia

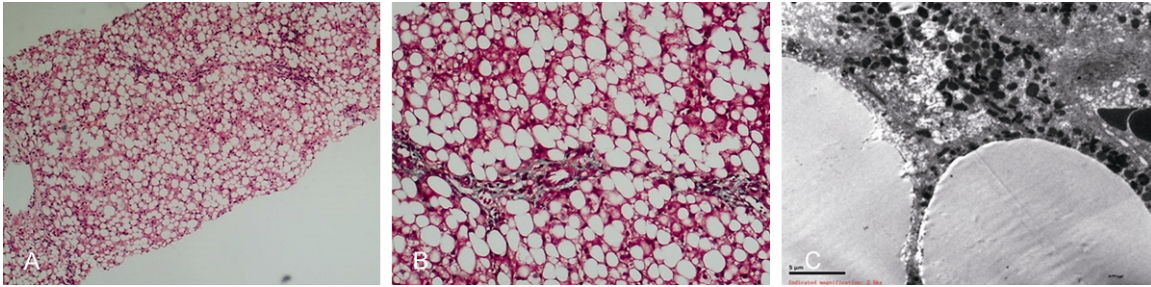


**Figure 2.** Nonalcoholic steatohepatitis revealed by liver biopsy. A. IHC found no detectable HBsAg, positive CK19 in bile duct epithelial cells, positive CD3 and CD20 in a small number of lymphocytes, and no obvious hyperplasia in small bile duct. B. The results of histopathology special stain masson trichrome test showed mild hyperplasia in fibrous tissue of small portal area (Figure 3B). C. Electron microscopy showed hepatocyte swelling and partial focal necrosis.

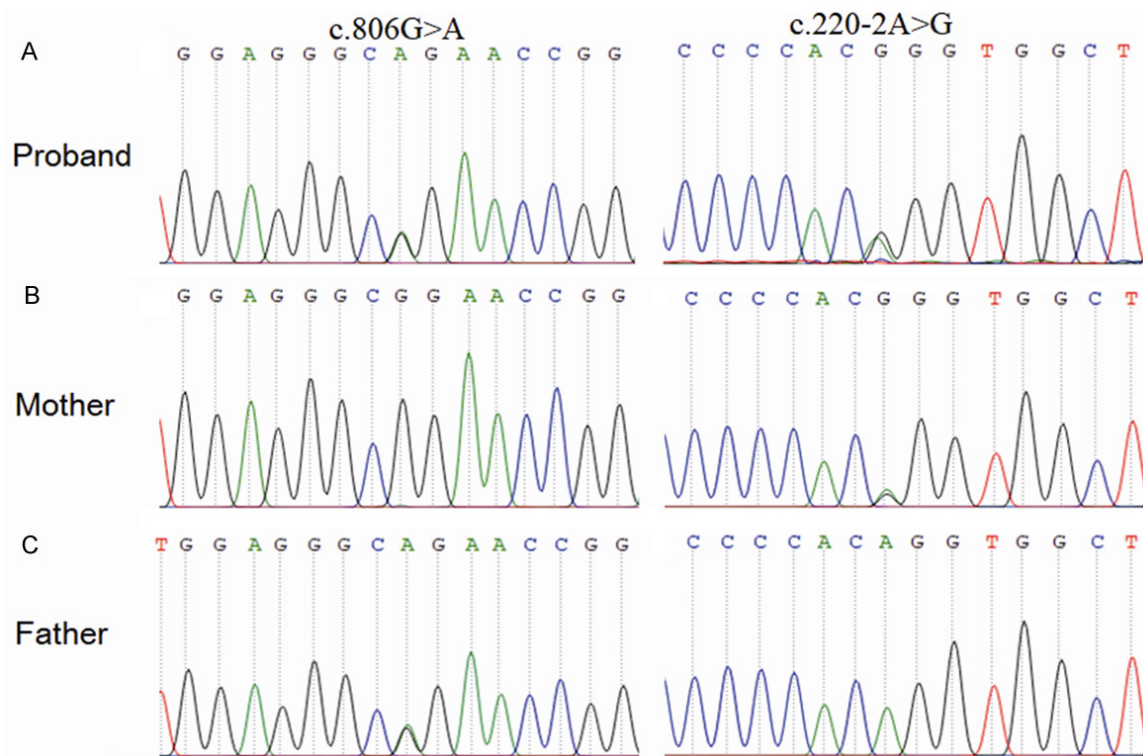


**Figure 3.** The mutations in *GPD1* gene for the proband (A), his mother (B) and his father (C).

(p.74\_96del) [15]. Therefore, it was possible to assume that the compound heterozygote was the etiology of the proband.

### *Sanger sequencing validated the candidate causative variants*

Sanger sequencing was undertaken in the family trio to confirm the candidate causative variants identified by WES. Sanger sequencing identified the compound heterozygote revealed by WES, which was inherited from the proband's

parents. His father carried one c.806G>A (p. R269Q) copy, while his mother was with the heterozygote mutation of c.220-2A>G (Figure 3). The results indicate that the variants contributed to the disease and the mutations in the proband were inherited from his parents.

### *Expression profile of GPD1 in human*

To further unravel the contribution of *GPD1* to the disease, we further obtained the 66 genes co-expressed with *GPD1* (Supplementary Table

## GPD1 causing transient hypertriglyceridemia

**Table 1.** Enrichment analysis for genes co-expressed with GPD1

Function item name	Number of hits	Expected number of hits	q-value	Resources
Triglyceride Biosynthesis	4	0.018	0.0000602	Reactome
Transcriptional regulation of white adipocyte differentiation	5	0.069	0.0000639	Reactome
Hormone-sensitive lipase (HSL)-mediated triacylglycerol hydrolysis	3	0.017	0.0034	Reactome
Synthesis of PA	3	0.017	0.0095	Reactome
Acyl chain remodeling of DAG and TAG	2	0.006	0.0482	Reactome
PPAR signaling pathway	6	0.056	0.000000764	KEGG
Glycerolipid metabolism	4	0.048	0.000196	KEGG
Glycerophospholipid metabolism	4	0.08	0.000913	KEGG

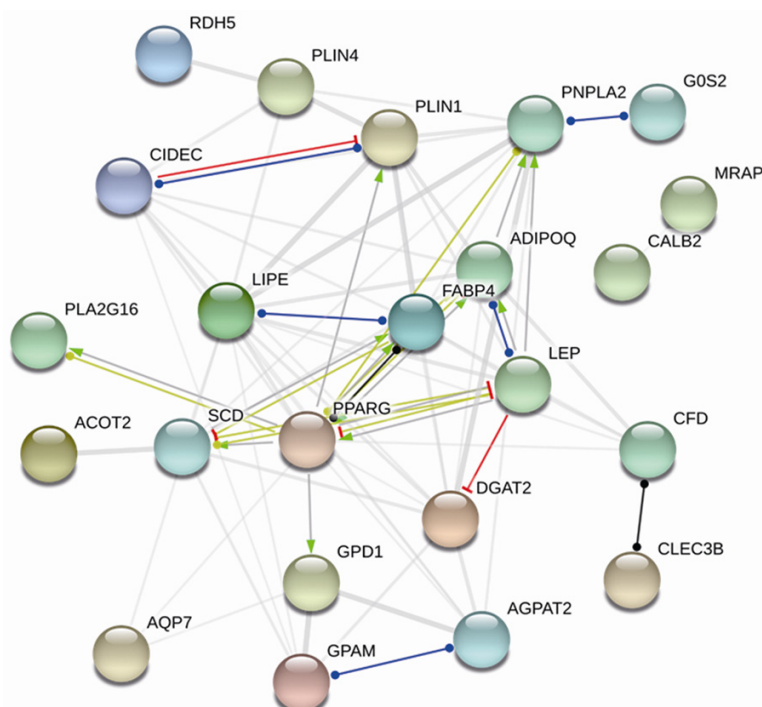


**Figure 4.** The PPI network of the genes co-expressed with GPD1.

1), and found that the genes were enriched in lipid metabolic related pathways (Table 1). Additionally, *GPD1* was found to be co-expressed with and regulated by Peroxisome proliferator-activated receptor gamma (PPARG, Supplementary Table 1, Figure 4), which is a nuclear receptor that binds peroxisome proliferators such as hypolipidemic drugs and fatty acids and controls the peroxisomal beta-oxidation pathway of fatty acids. Furthermore, genes co-expressed with *GPD1* could be enriched in PPAR signaling pathway. These results demonstrate that *GPD1* is involved in a network controlling fatty acids. In line with this, the truncating variants in *GPD1* could be possible to induce diseases associated with fatty acids metabolism

disorder, and thus its mutations could result in changes of triglyceridemia.

### Discussion

This study described a Chinese infant, who exhibited hepatosplenomegaly, non-alcoholic steatohepatitis, and HTGT1. Genetic sequencing revealed that the patient harbored heterozygous mutations, c.220-2A>G and c.806G>A (p.R269Q), in the *GPD1* gene. A previous report suggests that the c.220-2A>G mutation leads to aberrant splicing, causing an in-frame deletion of 23 amino acids (c.220\_288del, p.74\_96del) in *GPD1* protein [16]. Furthermore, the p.R269Q variant is predicted to be damaged and is reported to be humongous in one

patient with HTGT1, whose parents are carriers [2]. These findings suggested that both of the mutations may be pathogenic and responsible for the Chinese proband.

*GPD1* protein catalyzes the reversible redox conversion of dihydroxyacetone phosphate (DHAP) and NADH to L-a-glycerol 3-phosphate (G3P) and NAD<sup>+</sup>. Among the highly conserved residues that define the active site in GPD protein, Arg269 has been shown to be important for substrate recognition from the structures [16]. Additionally, the guanidine side chain of R269 interacts with Q295, and N270 interacts for the substrate phosphodianion. Furthermore, both function to optimize the apparent transi-

## GPD1 causing transient hypertriglyceridemia

tion-state stabilization provided by the cationic side chain of R269 [17]. So, the mutation p. R269Q was likely to be damage to the function of GPD1 and, therefore, could reduce the activity of GPD1.

However, it was strange to find an increase of TG in patients with *GPD1* mutation. Because GPD1 deficiency leads to a decrease of G3P, which is needed for TG synthesis in the liver [18]. To explain the clinical phenotype, the authors suggested that the peroxisomal pathway of DHAP acylation may be activated [1]. The genes co-expressed with *GPD1* could have been involved in the PPAR pathway, and activation of PPAR in mice and human is generally associated with a decrease in plasma triglycerides. Therefore, we further speculate that the PPAR pathway may also contribute to the phenotype of a low level G3P with high TG.

In a summary, compound heterozygous mutations, c.220-2A>G and c.806G>A (p.R269Q) in *GPD1* gene, were identified in a Chinese family affected by HTGT1. Furthermore, the two mutations had been both found in other patients reported previously and then suggested that they were responsible for the proband. We, therefore, show that WES is of great value in finding disease-caused mutations in monogenic diseases.

### Disclosure of conflict of interest

None.

**Address correspondence to:** Xianhua Zhang, Children's Medical Center, Hunan Provincial People's Hospital/First Affiliated Hospital of Hunan Normal University, 61 Jiefang West Road, Changsha 410005, Hunan, P. R. China. Tel: +86-10-83928300; E-mail: xi2019954jjiao@163.com

### References

- [1] Joshi M, Eagan J, Desai NK, Newton SA, Towne MC, Marinakis NS, Esteves KM, De Ferranti S, Bennett MJ, McIntyre A, Beggs AH, Berry GT and Agrawal PB. A compound heterozygous mutation in *GPD1* causes hepatomegaly, steatohepatitis, and hypertriglyceridemia. *Eur J Hum Genet* 2014; 22: 1229-1232.
- [2] Dionisi-Vici C, Shteyer E, Niceta M, Rizzo C, Pode-Shakked B, Chillemi G, Bruselles A, Semeraro M, Barel O, Eyal E, Kol N, Haberman Y,

Lahad A, Diomedi-Camassei F, Marek-Yagel D, Rechavi G, Tartaglia M and Anikster Y. Expanding the molecular diversity and phenotypic spectrum of glycerol 3-phosphate dehydrogenase 1 deficiency. *J Inher Metab Dis* 2016; 39: 689-695.

- [3] Basel-Vanagaite L, Zevit N, Har Zahav A, Guo L, Parathath S, Pasmanik-Chor M, McIntyre AD, Wang J, Albin-Kaplanski A, Hartman C, Marom D, Zeharia A, Badir A, Shoerman O, Simon AJ, Rechavi G, Shohat M, Hegele RA, Fisher EA and Shamir R. Transient infantile hypertriglyceridemia, fatty liver, and hepatic fibrosis caused by mutated *GPD1*, encoding glycerol-3-phosphate dehydrogenase 1. *Am J Hum Genet* 2012; 90: 49-60.
- [4] Brown LJ, Koza RA, Marshall L, Kozak LP and MacDonald MJ. Lethal hypoglycemic ketosis and glyceroluria in mice lacking both the mitochondrial and the cytosolic glycerol phosphate dehydrogenases. *J Biol Chem* 2002; 277: 32899-32904.
- [5] McKenna A, Hanna M, Banks E, Sivachenko A, Cibulskis K, Kernytsky A, Garimella K, Altshuler D, Gabriel S, Daly M and DePristo MA. The genome analysis toolkit: a MapReduce framework for analyzing next-generation DNA sequencing data. *Genome Res* 2010; 20: 1297-1303.
- [6] Wang K, Li M and Hakonarson H. ANNOVAR: functional annotation of genetic variants from high-throughput sequencing data. *Nucleic Acids Res* 2010; 38: e164.
- [7] Choi Y and Chan AP. PROVEAN web server: a tool to predict the functional effect of amino acid substitutions and indels. *Bioinformatics* 2015; 31: 2745-2747.
- [8] Reva B, Antipin Y and Sander C. Predicting the functional impact of protein mutations: application to cancer genomics. *Nucleic Acids Res* 2011; 39: e118.
- [9] Adzhubei IA, Schmidt S, Peshkin L, Ramensky VE, Gerasimova A, Bork P, Kondrashov AS and Sunyaev SR. A method and server for predicting damaging missense mutations. *Nat Methods* 2010; 7: 248-249.
- [10] van Dam S, Craig T and de Magalhaes JP. GeneFriends: a human RNA-seq-based gene and transcript co-expression database. *Nucleic Acids Res* 2015; 43: D1124-1132.
- [11] Szklarczyk D, Franceschini A, Wyder S, Forslund K, Heller D, Huerta-Cepas J, Simonovic M, Roth A, Santos A, Tsafou KP, Kuhn M, Bork P, Jensen LJ and von Mering C. STRING v10: protein-protein interaction networks, integrated over the tree of life. *Nucleic Acids Res* 2015; 43: D447-452.
- [12] Backes C, Keller A, Kuentzer J, Kneissl B, Comtesse N, Elnakady YA, Muller R, Meese E and

## GPD1 causing transient hypertriglyceridemia

- Lenhof HP. GeneTrail–advanced gene set enrichment analysis. *Nucleic Acids Res* 2007; 35: W186-192.
- [13] Li YL, Kang Y, Yang M, Zhou LP, Tian Z and Fu BY. Analysis of serum adiponectin level and related factors in nonalcoholic fatty liver disease. *Journal of China Medical University* 2009; 927-929.
- [14] Richards S, Aziz N, Bale S, Bick D, Das S, Gastier-Foster J, Grody WW, Hegde M, Lyon E, Spector E, Voelkerding K, Rehm HL and Committee ALQA. Standards and guidelines for the interpretation of sequence variants: a joint consensus recommendation of the American college of medical genetics and genomics and the association for molecular pathology. *Genet Med* 2015; 17: 405-424.
- [15] Li N, Chang G, Xu Y, Ding Y, Li G, Yu T, Yao R, Li J, Shen Y, Wang X and Wang J. Biallelic mutations in GPD1 gene in a Chinese boy mainly presented with obesity, insulin resistance, fatty liver, and short stature. *Am J Med Genet A* 2017; 173: 3189-3194.
- [16] Ou X, Ji C, Han X, Zhao X, Li X, Mao Y, Wong LL, Bartlam M and Rao Z. Crystal structures of human glycerol 3-phosphate dehydrogenase 1 (GPD1). *J Mol Biol* 2006; 357: 858-869.
- [17] He R, Reyes AC, Amyes TL and Richard JP. Enzyme architecture: the role of a flexible loop in activation of glycerol-3-phosphate dehydrogenase for catalysis of hydride transfer. *Biochemistry* 2018; 57: 3227-3236.
- [18] Declercq PE, Debeer LJ and Mannaerts GP. Role of glycerol 3-phosphate and glycerophosphate acyltransferase in the nutritional control of hepatic triacylglycerol synthesis. *Biochem J* 1982; 204: 247-256.

## GPD1 causing transient hypertriglyceridemia

**Supplementary Table 1.** The genes co-expressed with GPD1

Ensembl Gene ID	Gene Symbol	Mutual Rank	Pearson Correlation	BioType	Chromosome	Chromosome Start	Chromosome End	Annotation
ENSG00000167588	GPD1	0	1	Protein_coding	12	50497602	50505102	Glycerol-3-phosphate dehydrogenase 1 (soluble)
ENSG00000187288	CIDEA	1	0.98	Protein_coding	3	9908398	9921938	Cell death-inducing dffa-like effector c
ENSG00000166819	PLIN1	2	0.97	Protein_coding	15	90207596	90222658	Perilipin 1
ENSG00000133317	LGALS12	2.4	0.95	Protein_coding	11	63273556	63284246	Lectin, galactoside-binding, soluble, 12
ENSG00000167676	PLIN4	2.8	0.95	Protein_coding	19	4502204	4517716	Perilipin 4
ENSG00000169692	AGPAT2	3.9	0.95	Protein_coding	9	1.4E+08	1.4E+08	1-acylglycerol-3-phosphate O-acyltransferase 2
ENSG00000042445	RETSAT	2.6	0.94	Protein_coding	2	85569211	85581743	Retinol saturase (all-trans-retinol 13,14-reductase)
ENSG00000174697	LEP	4.9	0.94	Protein_coding	7	1.28E+08	1.28E+08	Leptin
ENSG00000181092	ADIPOQ	5.2	0.93	Protein_coding	3	1.87E+08	1.87E+08	Adiponectin, C1Q and collagen domain containing
ENSG00000062282	DGAT2	6.3	0.93	Protein_coding	11	75470557	75512579	Diacylglycerol O-acyltransferase 2
ENSG00000170323	FABP4	7.1	0.93	Protein_coding	8	82390654	82395498	Fatty acid binding protein 4, adipocyte
ENSG00000135917	SLC19A3	3.3	0.92	Protein_coding	2	2.29E+08	2.29E+08	Solute carrier family 19 (thiamine transporter), member 3
ENSG00000135437	RDH5	9.2	0.92	Protein_coding	12	56114151	56118489	Retinol dehydrogenase 5 (11-cis/9-cis)
ENSG00000079435	LIPE	8.8	0.91	Protein_coding	19	42905659	42931578	Lipase, hormone-sensitive
ENSG00000165269	AQP7	9.2	0.91	Protein_coding	9	33384765	33402643	Aquaporin 7
ENSG00000135447	PPP1R1A	9.5	0.9	Protein_coding	12	54969171	54982443	Protein phosphatase 1, regulatory (inhibitor) subunit 1A
ENSG00000119673	ACOT2	9.8	0.9	Protein_coding	14	74034324	74042357	Acyl-CoA thioesterase 2
ENSG00000158571	PFKFB1	4.2	0.89	Protein_coding	X	54959394	55024967	6-phosphofructo-2-kinase/fructose-2,6-biphosphatase 1
ENSG00000123689	GOS2	7.7	0.89	Protein_coding	1	2.1E+08	2.1E+08	G0/G1 switch 2
ENSG00000170262	MRAP	10.1	0.89	Protein_coding	21	33664124	33687095	Melanocortin 2 receptor accessory protein
ENSG00000184811	TUSC5	13.8	0.89	Protein_coding	17	1182957	1204281	Tumor suppressor candidate 5
ENSG00000119927	GPAM	11.2	0.87	Protein_coding	10	1.14E+08	1.14E+08	Glycerol-3-phosphate acyltransferase, mitochondrial
ENSG00000172137	CALB2	8.3	0.86	Protein_coding	16	71392616	71424341	Calbindin 2
ENSG00000099194	SCD	10.4	0.86	Protein_coding	10	1.02E+08	1.02E+08	Stearoyl-CoA desaturase (delta-9-desaturase)
ENSG00000056998	GYG2	10.5	0.86	Protein_coding	X	2746829	2800859	Glycogenin 2
ENSG00000131471	AOC3	12.2	0.86	Protein_coding	17	41003201	41010147	Amine oxidase, copper containing 3
ENSG00000186458	DEFB132	15.5	0.86	Protein_coding	20	238377	241737	Defensin, beta 132
ENSG00000262179		17.7	0.86					
ENSG00000197766	CFD	23.1	0.84	Protein_coding	19	859453	863453	Complement factor D (adipsin)
ENSG00000176485	PLA2G16	15.5	0.83	Protein_coding	11	63340667	63384355	Phospholipase A2, group XVI
ENSG00000267272	LINC01140	15.7	0.83	Lincrna	1	87595448	87634881	Long intergenic non-protein coding RNA 1140
ENSG00000271239		26.4	0.83					
ENSG00000176720	BOK	5.9	0.82	Protein_coding	2	2.42E+08	2.43E+08	BCL2-related ovarian killer
ENSG00000042286	AIFM2	11.3	0.82	Protein_coding	10	71857979	71892690	Apoptosis-inducing factor, mitochondrion-associated, 2
ENSG00000163710	PCOLCE2	18.4	0.82	Protein_coding	3	1.43E+08	1.43E+08	Procollagen C-endopeptidase enhancer 2
ENSG00000189129	PLAC9	29.3	0.82	Protein_coding	10	81891438	81905115	Placenta-specific 9
ENSG00000134463	ECHDC3	14.1	0.81	Protein_coding	10	11784365	11806069	Enoyl CoA hydratase domain containing 3
ENSG00000123612	ACVR1C	15.1	0.81	Protein_coding	2	1.58E+08	1.58E+08	Activin A receptor, type IC

## GPD1 causing transient hypertriglyceridemia

ENSG00000245812		15.3	0.81						
ENSG00000181997		19	0.81	Unprocessed_pseudogene	9	69633978	69650004	Aquaporin 7 pseudogene 2	
ENSG00000177666	PNPLA2	20.2	0.81	Protein_coding	11	818902	825573	Patatin-like phospholipase domain containing 2	
ENSG00000184601	C14orf180	21.5	0.81	Protein_coding	14	1.05E+08	1.05E+08	Chromosome 14 open reading frame 180	
ENSG00000157150	TIMP4	24	0.81	Protein_coding	3	12194551	12200851	TIMP metalloproteinase inhibitor 4	
ENSG00000272734		36.5	0.81	Processed_transcript	10	88725102	88731068	ADIRF antisense RNA 1	
ENSG00000230148	HOXB-AS1	9.4	0.8	Antisense	17	46620913	46628610	HOXB cluster antisense RNA 1	
ENSG00000229436		13.4	0.8						
ENSG00000186205	1-Mar	18.1	0.8	Protein_coding	1	2.21E+08	2.21E+08	Mitochondrial amidoxime reducing component 1	
ENSG00000132170	PPARG	28	0.8	Protein_coding	3	12328867	12475855	Peroxisome proliferator-activated receptor gamma	
ENSG00000008394	MGST1	19.1	0.79	Protein_coding	12	16500076	16762193	Microsomal glutathione S-transferase 1	
ENSG00000103876	FAH	20.8	0.79	Protein_coding	15	80444832	80479288	Fumarylacetoacetate hydrolase (fumarylacetoacetase)	
ENSG00000186466		22.1	0.79	Unprocessed_pseudogene	9	67272038	67289492	Aquaporin 7 pseudogene 1	
ENSG00000228695	CES1P1	25.2	0.79	Transcribed_unprocessed_pseudogene	16	55794460	55828070	Carboxylesterase 1 pseudogene 1	
ENSG00000130876	SLC7A10	25.5	0.79	Protein_coding	19	33699570	33716756	Solute carrier family 7 (neutral amino acid transporter light chain, asc system), member 10	
ENSG00000159884	CCDC107	25.9	0.79	Protein_coding	9	35658301	35661508	Coiled-coil domain containing 107	
ENSG00000166823	MESP1	30.3	0.79	Protein_coding	15	90291892	90294541	Mesoderm posterior 1 homolog (mouse)	
ENSG00000171227	TMEM37	10.6	0.78	Protein_coding	2	1.2E+08	1.2E+08	Transmembrane protein 37	
ENSG00000163815	CLEC3B	35.4	0.78	Protein_coding	3	45043040	45077563	C-type lectin domain family 3, member B	
ENSG00000227591		39.9	0.78						
ENSG00000108960	MMD	15.2	0.77	Protein_coding	17	53469974	53499353	Monocyte to macrophage differentiation-associated	
ENSG00000254211		37.6	0.77						
ENSG00000197582		41.3	0.77	Processed_pseudogene	X	13396854	13397459	Glutathione peroxidase pseudogene 1	
ENSG00000224525		42.4	0.77						
ENSG00000150594	ADRA2A	17.9	0.76	Protein_coding	10	1.13E+08	1.13E+08	Adrenoceptor alpha 2A	
ENSG00000151632	AKR1C2	32.7	0.76	Protein_coding	10	5029967	5060223	Aldo-keto reductase family 1, member C2	
ENSG00000174899	C3orf55	38.6	0.76	Protein_coding	3	1.57E+08	1.57E+08	Chromosome 3 open reading frame 55	
ENSG00000106823	ECM2	16.2	0.75	Protein_coding	9	95256365	95298937	Extracellular matrix protein 2, female organ and adipocyte specific	
ENSG00000115459	ELMOD3	30.2	0.75	Protein_coding	2	85581517	85618875	ELMO/CED-12 domain containing 3	